ANNUAL REVIEWS

Annual Review of Condensed Matter Physics

Quantum Turbulence in Quantum Gases

L. Madeira,[1] M.A. Caracanhas,[1] F.E.A. dos Santos,[2] and V.S. Bagnato[1]

[1]Instituto de Física de São Carlos, Universidade de São Paulo, São Carlos 13560-970, Brazil; email: madeira@ifsc.usp.br

[2]Departamento de Física, Universidade Federal de São Carlos, São Carlos 13565-905, Brazil

Annu. Rev. Condens. Matter Phys. 2020. 11:37–56

The *Annual Review of Condensed Matter Physics* is online at conmatphys.annualreviews.org

https://doi.org/10.1146/annurev-conmatphys-031119-050821

Keywords

Bose–Einstein condensate, BEC, ultracold gases, quantized vortex, vortex reconnection, energy cascade

Abstract

Turbulence is characterized by a large number of degrees of freedom, distributed over several length scales, that result in a disordered state of a fluid. The field of quantum turbulence deals with the manifestation of turbulence in quantum fluids, such as liquid helium and ultracold gases. We review, from both experimental and theoretical points of view, advances in quantum turbulence focusing on atomic Bose–Einstein condensates. We also explore the similarities and differences between quantum and classical turbulence. Last, we present challenges and possible directions for the field. We summarize questions that are being asked in recent works, which need to be answered in order to understand fundamental properties of quantum turbulence, and we provide some possible ways of investigating them.

1. INTRODUCTION

CT: classical turbulence

QT: quantum turbulence

BECs: Bose–Einstein condensates

BS: Biot–Savart

GP: Gross–Pitaevskii

Turbulence is characterized by a large number of degrees of freedom interacting nonlinearly, over a substantial range of scales, to produce a disordered state both in space and time. Many aspects of classical turbulence (CT) are not well understood, so tackling its quantum version, quantum turbulence (QT), seems ambitious. It turns out that dealing with turbulence in quantum fluids might be easier than in its classical counterpart due to the fact that the vortex circulation is quantized in the former and continuous in the latter. The advances in trapping, cooling, and tuning the interparticle interactions in atomic Bose–Einstein condensates (BECs) make them excellent candidates for studying QT due to the amount of control that one can exert over these systems.

Despite the intrinsic difficulties of this problem, much progress has been accomplished (1–3). A milestone was the first observation of turbulence in a trapped BEC (4) and its signature self-similar expansion. The occurrence of an energy cascade, demonstrated by the presence of a power law in the energy spectrum $E \propto k^{-\delta}$, can be considered an important step toward the understanding of turbulence in confined systems (5–7).

A few words about the scope of this review are in order. In this work, we focus on QT in trapped BECs. Comparisons with turbulence in liquid helium are made when pertinent, but a full review of the subject is beyond the scope of this article. The same can be said about CT.

This review is structured as follows: A very brief introduction to quantum gases is given in Section 2. In Section 3, we present the main aspects of QT. We begin with definitions of turbulence and QT in Section 3.1. The picture of a tangle of vortices giving rise to turbulence is first introduced in Section 3.2. In Section 3.3, we contrast aspects of CT and QT and provide brief accounts of both. Some models used to explore QT, namely the Biot–Savart (BS) and Gross–Pitaevskii (GP) models, are introduced in Section 3.4. Wave turbulence is discussed in Section 3.5. Section 3.6 deals with one mechanism that is believed to be essential to QT: vortex reconnections. Some aspects of two-dimensional turbulence, which is substantially different from its three-dimensional counterpart, are presented in Section 3.7. Section 3.8 contains topics that are not related to the usual single-component BECs employed in the study of QT, namely bosonic mixtures and fermionic systems. Section 4 summarizes experimental achievements, describing important aspects of turbulence observed in quantum gases in 3D and 2D. We emphasize the recent developments in our group, and we show how the experiments performed in our laboratories relate to the research on QT being performed worldwide. Finally, in Section 5, we present some challenges and future issues that, in our opinion, the field must face.

2. QUANTUM GASES

2.1. Bose–Einstein Condensates

Bose–Einstein condensation corresponds to the macroscopic occupation of the lowest-energy quantum state by the particles of a system. This occurs if the temperature T of the system is cooled below a critical temperature T_c. Bose–Einstein condensation occurs when the mean interparticle distance $\bar{l} = (\bar{\rho})^{-1/3}$, $\bar{\rho}$ being the number density of N particles in a volume V, is comparable with the de Broglie wavelength $\lambda_{dB} = h/(mv)$, where h is Planck's constant, m is the mass of the atoms, and $v = \sqrt{k_B T/m}$ is their thermal velocity, k_B being the Boltzmann constant. Imposing $\lambda_{dB} \sim \bar{l}$ implies that a homogeneous gas undergoes a Bose–Einstein condensation at a temperature $T_c \sim h^2 \rho^{2/3}/(mk_B)$. This simple qualitative argument differs from the accurate result (8) only by a factor of $\approx$3.3. The first experimental realizations of Bose–Einstein condensation in dilute gases were achieved in 1995 (9–11), and currently several laboratories around the world produce BECs on a daily basis. Most of these experiments are performed on inhomogeneous gases in harmonic

trapping potentials. Then, the critical temperature (8) is given by $T_c = 0.15\hbar\bar{\omega}N^{1/3}/k_B$, where $\bar{\omega} = (\omega_x\omega_y\omega_z)^{1/3}$ is the geometric mean of the three Cartesian trapping frequencies ω_i, where $i = x, y, z$. Trapping techniques usually employ magnetic fields or optical means. The extremely low temperatures are achieved by laser cooling and evaporation. One feature of experiments with cold atomic gases that led to rapid advances in the field is the ability to control interactions in the systems. The interatomic interactions and trapping potentials can be changed by modifying external parameters with unprecedented control, such as the applied electromagnetic fields.

2.2. Superfluid Helium

Liquid He was first produced in 1908, and 20 years later scientists noticed that liquid He had two very distinct phases, HeI and HeII, with a singularity in the specific heat, called λ-point, between them (12). The behavior of liquid HeI was the same as regular liquids, whereas HeII displayed unusual mechanical and thermal properties at low temperatures. Progress was made with the discovery of superfluidity (13, 14), flow without viscous dissipation, in direct analogy with the lack of resistance in a superconductor.

London was the first to connect HeII with Bose–Einstein condensation (15), proposing a macroscopic wave function for the condensed atoms. However, more attention was given to the phenomenological two-fluid model introduced by Tisza (16). According to this model, liquid He is composed of a normal and a superfluid part, each of them with its own density and velocity field. The normal component behaves as a regular fluid, whereas the superfluid has no entropy and flows without friction. Later, Landau formalized the model (17), which was successful in explaining a variety of properties and effects in liquid He. However, a major problem with the two-fluid model is that it assumes zero superfluid vorticity, the vorticity being the curl of the velocity field. This is because, in the absence of dissipations, the velocity field should be conservative, and thus it can be written as the gradient of a field, and the curl of a gradient is zero ($\boldsymbol{\omega} = \nabla \times \mathbf{v} = \nabla \times \nabla\phi = 0$). Experiments, however, showed clear indications that the vorticity did not vanish.

2.3. Quantized Vortices

Because Bose–Einstein condensation corresponds to the collective occupation of the zero-momentum state, then a macroscopic wave function can be used for the N condensed atoms, $\psi(\mathbf{r}, t) = \sqrt{\rho(\mathbf{r}, t)}\exp[iS(\mathbf{r}, t)]$, where $\rho(\mathbf{r}, t) = |\psi(\mathbf{r}, t)|^2$ is the condensed density, $S(\mathbf{r}, t)$ is its phase, and the normalization is given by $\int \mathrm{d}^3\mathbf{r}|\psi(\mathbf{r}, t)|^2 = N$. The probability current is given by $\mathbf{j} = \hbar/(2mi)(\psi^*\nabla\psi - \psi\nabla\psi^*) = \rho(\hbar/m)\nabla S$ (we have omitted the spatial and time dependencies hereafter for brevity). This is a flux of the density ρ that flows with velocity $\mathbf{v} = (\hbar/m)\nabla S$, where $\mathbf{j} = \rho\mathbf{v}$. A consequence is that, when S has continuous first and second derivatives, the velocity field is irrotational, $\nabla \times \mathbf{v} = 0$. In the presence of a vortex line, a line singularity where $\mathbf{v}$ diverges, this does not hold. Thus, a vortex-free velocity field is irrotational.

The circulation Γ around a closed path C is given by $\Gamma = \oint_C \mathrm{d}\mathbf{r} \cdot \mathbf{v}$. The macroscopic wave function has to be single-valued, which requires the phase to change by $2\pi n$, where n is an integer, and it is often called the charge of the vortex, when going around the contour. This gives rise to the quanta of circulation $\kappa = h/m$,

$$\Gamma = \oint_C \mathrm{d}\mathbf{r} \cdot \mathbf{v} = \frac{\hbar}{m} 2\pi n = n\kappa. \qquad 1.$$

This led Onsager (18) and Feynman (19) to introduce the quantization of the vorticity in superfluid He. A vortex is an excitation of the system; thus, it is a state with higher energy than the ground

state. The energy is proportional to the square of the vortex charge, $E \propto n^2$, thus it is energetically favorable to have n single-charged vortices rather than one n-charged vortex (20).

3. QUANTUM TURBULENCE

3.1. Nomenclature

The term QT was first used in 1982 by Barenghi in his Ph.D. thesis (21). Donnelly & Swanson, who adopted the term in 1986 (22), were responsible for the shift from the commonly used superfluid to QT. This change was not simply a matter of nomenclature; it showed that turbulence had more to do with the quantization of vortices than the lack of viscosity of superfluids. Indeed, experiments later showed that turbulence would decay even in the case of vanishing viscosity. The very pertinent question of where the energy goes if there is no friction was answered by the realization that vortices decay into sound, as seen in experiments with two-dimensional BECs (23) and numerical simulations using the GP equation in 2D (24) and 3D (25).

Having justified the term QT, we still have to define turbulence. A definition that seems to be accepted is that it is a state of spatially and temporally disordered flow, with a large number of degrees of freedom that interact nonlinearly. Usually, by nonlinear interaction we mean the term $(\mathbf{v} \cdot \nabla)\mathbf{v}$ in the classical Euler equation,

$$\frac{\partial \mathbf{v}}{\partial t} + (\mathbf{v} \cdot \nabla)\mathbf{v} = -\frac{1}{\rho}\nabla p, \qquad 2.$$

where p is the pressure. The equation above is essentially Newton's second law for the continuum. The nonlinear term arises from writing the force per unit volume acting on a fluid parcel that is moving rather than being at a fixed point in space. As we discuss below, this equation can be seen as a particular case of the (incompressible) Navier–Stokes equation with zero viscosity.

3.2. From Vortices to Turbulence

Vortex lines can sustain helical deformations, called Kelvin waves, that move them from a straight orientation. Also, two lines that approach each other can reconnect and form a cusp, which relaxes into Kelvin waves. Disordered combinations of vortex lines can be a manifestation of QT, as proposed by Feynman (19). The subsequent work done by Hall & Vinen (26, 27) motivated the study of QT using ^{4}He. The recent progress of QT in the context of trapped BECs came with striking discoveries. For example, under appropriate conditions, statistical properties of CT may arise. One of them is the Kolmogorov scaling of the energy spectrum ($E \propto k^{-5/3}$), which suggests an energy cascade from large to small length scales. This defines what is called Kolmogorov turbulence, which is found in a specific inertial range as long as there is constant injection of energy at large length scales. This requires a self-similar process in which large bundles of vortices transfer energy to smaller bundles, until the energy reaches a single vortex.

Numerical simulations showed that if QT obeys the energy spectrum of the Kolmogorov turbulence, the vortex tangle contains transient vortex bundles (vortices with the same orientation) together with many random vortices (28). These structures are responsible for the large-scale, small k, flows. Although the Kolmogorov scaling has been observed in experiments, these vortex bundles have not. Kolmogorov turbulence has been observed in He at low and high temperatures, $T \ll T_c$ and $T \sim T_c$ (where T_c is the critical temperature, as defined in Section 2.1), respectively. At high temperatures, the normal fluid dominates, so CT is expected. However, at low temperatures the situation is more interesting. Energy transfer occurs because of the nonlinear term $(\mathbf{v} \cdot \nabla)\mathbf{v}$ in the Euler equation (Equation 2). This helps to connect both QT and CT.

Experiments (29) showed that, besides Kolmogorov turbulence, there is another regime where superfluid ^{4}He displays a different kinetic energy spectrum. This different kind of turbulence, called Vinen or ultraquantum turbulence, was observed in superfluid He by controlling the injections of vortex rings in the system. A diagnostic to differentiate both kinds of turbulence is the temporal decay of the vortex line density $L(t)$. For short injections of vortex rings, this produced a regime with $L(t) \propto t^{-1}$, whereas long injections yielded $L(t) \propto t^{-3/2}$. Numerical simulations of the experiment (30) showed that Vinen turbulence, corresponding to $L(t) \propto t^{-1}$, has a spectrum $E \propto k^{-1}$ for large k (in the hydrodynamical range), whereas the $-5/3$ Kolmogorov scaling was observed for the $L(t) \propto t^{-3/2}$ regime. It is understood that Vinen turbulence is set apart from Kolmogorov's because of the random tangles of vortices that lead to an absence of large-scale flow structures.

The question of whether turbulence in trapped BECs is Kolmogorov, Vinen, a combination of both, or neither, is still unsettled. However, two vortices in an orthogonal orientation or one doubly charged vortex may decay and display a Kolmogorov energy spectrum (31). Numerical models using the GP equation also suggest that trapped BECs should show Kolmogorov turbulence (32).

One last distinction should be made. Stationary turbulence in three-dimensional (two-dimensional) systems requires constant energy injection in large (small) length scales, which cascades to small (large) scales and is dissipated with the same rate as that of injection. In nature, stationary turbulent systems decay when the energy input stops, characterizing what we call decaying turbulence.

3.3. Classical Versus Quantum Turbulence

One of the most important differences between CT and QT is the quantization of the circulation (see Section 2.3). In this sense, the quantum version of the problem is easier to handle because circulation, which is continuous in the classical case, can only take a discrete set of values. Regular fluids are viscous; thus, without a constant energy input, turbulence decays. At sufficient low temperatures, the thermal component of the trapped gases is negligible, and it can be considered a pure superfluid. Even in that scenario, turbulence decays without constant energy injection because of sound waves inside and at the surface of the condensate.

Trapped BECs also show some interesting features regarding the amount of control exerted on experiments. The number of atoms, trapping parameters, and interatomic interactions can be varied to produce the desired regimes. The drawback is that this freedom often complicates the comparison between two sets of experiments.

The characteristic length scales are different when we compare CT and QT and, furthermore, the range available in each case also differs. In classical fluids, vortices can be as large as the typical length scale of the system D. For a typical BEC, the vortex core is comparable to the healing length ξ, and the distance between the vortices is a few times ξ. In **Table 1**, we show some similarities and differences between CT and QT.

3.3.1. Classical turbulence. The generalization of Euler's equation (Equation 2) is the Navier–Stokes equation. In the case of a solenoidal incompressible fluid, it can be written as

$$\frac{\partial \mathbf{v}}{\partial t} + (\mathbf{v} \cdot \nabla)\mathbf{v} = -\frac{1}{\rho}\nabla p + \nu \nabla^2 \mathbf{v} + \mathbf{g} \text{ and } \nabla \cdot \mathbf{v} = 0, \qquad 3.$$

where $\mathbf{g}$ stands for the external forces. Reynolds studied the transition from laminar to turbulent flows in a pipe. He found that the transition required the Reynolds number $Re = vD/\nu$, which quantifies the intensity of the turbulence (where v is the flow velocity at a length scale D, and ν is

Table 1 Comparison between classical and quantum turbulence in superfluid helium and trapped Bose–Einstein condensates

	Classical	Quantum	
		^{4}He	Trapped BECs
Vorticity	Continuous	Discrete and quantized	
Range of scales	Forcing scale to Kolmogorov length	Forcing scale to intervortex distance/vortex line length	
Dissipation	Viscosity	Sound waves	
Model	Navier–Stokes equation	Two fluid	Gross–Pitaevskii
Homogeneity	Homogeneous	Homogeneous	Nonhomogeneous
Threshold to turbulence given by	Reynolds number	Intervortex distance, vortex line length, system size	
Turbulence type	Hydrodynamical, wave	Hydrodynamical, wave, Vinen	

the kinematic viscosity of the fluid and can be seen as the ratio of inertial to viscous forces), to be above a certain threshold number.

The concept of energy cascade came in the 1920s with Lewis Richardson, who knew that a turbulent steady state required a constant energy injection at large length scales and that the energy was to be dissipated with the same rate at small length scales. The intermediary range, called inertial range, was characterized by being independent of the viscosity. In the 1940s, Kolmogorov formalized the concept of an energy cascade with a self-similar behavior of the turbulent flow. In the simplest case of an isotropic and homogeneous steady state, the energy goes from the largest length scale D to the smallest one η, with a constant dissipation rate ε. The Reynolds number connects these length scales, $\eta/D \approx Re^{-3/4}$. Kolmogorov suggested that some aspects of turbulence are universal. Instead of working in real space, it is convenient to go to the momentum space to describe the cascade as a function of wavenumbers $k = 2\pi/r$. In the inertial range, Kolmogorov showed that the kinetic energy is given by

$$E_k = C\varepsilon^{2/3}k^{-5/3}, \qquad 4.$$

where C is dimensionless and of order one.

Kolmogorov's law (Equation 4) describes three-dimensional flow. There are only a few examples of physical systems in which flow is truly 2D; in most cases two-dimensional flow is used as an approximation to a three-dimensional problem, or as building blocks to anisotropic turbulence in 3D. Nevertheless, two-dimensional CT is completely different from its three-dimensional counterpart. In 1967, Kraichnan showed that, in 2D, the energy flows from small to large length scales, in the opposite direction of the three-dimensional case. The same exponent, $E \propto k^{-5/3}$, is found but due to an inverse energy cascade. This occurs simultaneously with a forward cascade of the enstrophy, a quantity that measures the variance of the vorticity (the integral of the square of the vorticity over a surface S in the xy-plane, $\varepsilon(\boldsymbol{\omega}) = \int_S |\boldsymbol{\omega}|^2 \mathrm{d}S$), which makes the energy spectrum $E \propto k^{-3}$ for large momenta.

3.3.2. Quantum turbulence. The visualization of the tangle of vortex lines that constitute turbulence in a trapped BEC is very difficult, thus much of the progress made has relied on numerical simulations. In liquid He experiments, the determination of the vortex line density L is more straightforward, and it can be used as a measure of both the intensity of the QT and the distance between vortices, $l \approx L^{-1/2}$.

Not all turbulent states that have been studied correspond to the Kolmogorov scaling. They can be of the Vinen kind (33), but it also depends on how the excitations are performed. If the

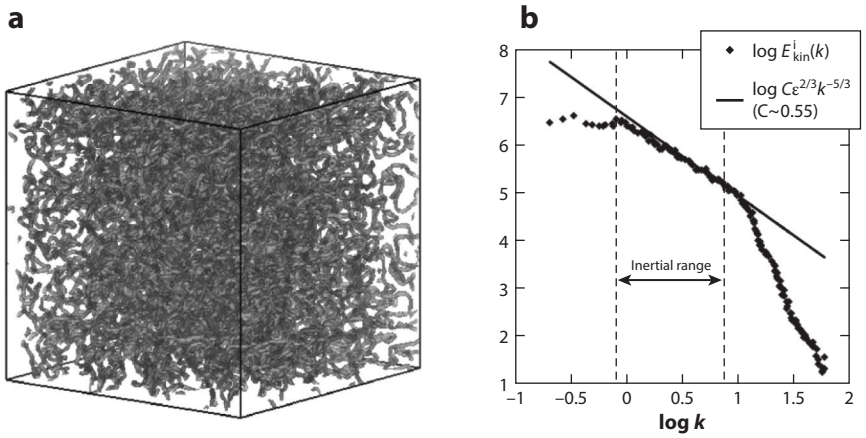

Figure 1

(*a*) Vortex tangle. (*b*) Spectrum of the incompressible kinetic energy for the turbulent regime. The points correspond to an ensemble average of 50 configurations, whereas the curve stands for the Kolmogorov law. Figure adapted with permission from Reference 1; Copyright 2008 The Physical Society of Japan.

superfluid is thermally driven, then it lacks energy at the largest scales and it displays $E \propto k^{-1}$ for large momenta (34). However, if the superfluid is driven by a turbulent normal fluid, then the energy spectrum is $E \propto k^{-5/3}$, as is the case for Kolmogorov turbulence (34). **Figure 1*a*** shows a vortex tangle in a homogeneous condensate, obtained from simulations (1); the Kolmogorov scaling is shown in **Figure 1*b***.

As we have been arguing throughout this review, one of the reasons for the complexity of QT comes from the large range of length, or conversely momentum, scales available. For the following discussion, let us define $k_l = 2\pi/l$ and $k_\xi = 2\pi/\xi$, wavenumbers corresponding to the intervortex distance and healing length, respectively. Discussions, so far, have been restricted to the hydrodynamical scale $k \ll k_l$. Now let us focus on the range of $k_l < k < k_\xi$, k_ξ being the limiting scale because vortices cannot bend on scales shorter than the vortex core radius, of order of ξ. It is understood that Kelvin waves produce increasingly shorter wavelengths until the angular frequency of the wave is fast enough to radiate sound; this is a process called Kelvin cascade. Different theories exist for the energy spectrum of this cascade, Kozik & Svistunov (35) obtained $E \propto k^{-7/5}$, whereas L'vov & Nazarenko (36) predicted $E \propto k^{-5/3}$. It is still unclear which of the exponents is correct; however, recent studies (37–39) support the spectrum proposed by L'vov & Nazarenko. Another possibility is that there is a bottleneck between the Kolmogorov and Kelvin cascades, which changes the shape of the energy spectrum around $k \approx k_l$ (40). This bottleneck is due to the faster rate at which energy flows down the three-dimensional Kolmogorov cascade, compared to the slower rate at which energy moves down the one-dimensional Kelvin cascade. A different approach, by supposing a smooth transition between the two cascades, has been suggested (41, 42).

3.4. Theoretical Models

Theoretical investigations of turbulent quantum fluids take place within some established framework. In the following, we present two widely employed theoretical models, the Biot–Savart model and the Gross–Pitaevskii equation.

VRs: vortex reconnections

3.4.1. The Biot–Savart model. First introduced by Schwarz (43), the BS model parameterizes the vortex line by the curve $s(\zeta, t)$, ζ being the arclength and t the time. Its name is inspired by the analogy with magnetic fields. In this model, the velocity is written as the curl of a vector potential $\mathbf{A}$, $\mathbf{v} = \nabla \times \mathbf{A}$. The vorticity then obeys the Poisson equation, $\nabla^2 \mathbf{A} = -\boldsymbol{\omega}$, with a solution given by

$$\mathbf{A}(\mathbf{r}) = \frac{1}{4\pi} \int \mathrm{d}^3\mathbf{r}' \frac{\boldsymbol{\omega}(\mathbf{r}')}{|\mathbf{r} - \mathbf{r}'|}, \qquad 5.$$

for a vortex core located at $\mathbf{r}$. The vorticity has a constant intensity along the vortex core, hence $\boldsymbol{\omega}(\mathbf{r}')\mathrm{d}^3\mathbf{r} = \kappa \mathrm{d}\boldsymbol{\ell}$, which allows the integration to be performed over a line, $1/(4\pi) \int \mathrm{d}\boldsymbol{\ell}\, \kappa/|\mathbf{r} - \mathbf{r}'|$. Notice that $\mathbf{A}$ describes an incompressible field, $\nabla \cdot \mathbf{v} = \nabla \cdot \nabla \times \mathbf{A} = 0$; however, a quantum fluid may have a compressible part that is not described in this model. Simulations employing this vector potential are computationally expensive. Instead, the velocity field may be replaced by $\mathbf{v}_{\mathrm{LIA}} = (\kappa/4\pi R)\ln(R/\zeta)(\mathbf{s}' \times \mathbf{s}'')$, where the primes stand for derivatives taken with respect to the arclength, $\mathbf{s}' = \mathrm{d}\mathbf{s}/\mathrm{d}\zeta$ (44). This is called local induction approximation owing to the fact that nonlocal contributions to the integral are neglected. Vortex reconnections (VRs), first introduced in Section 3.2 and discussed in Section 3.6, are essential for QT simulations. These are absent in the BS model and need to be included ad hoc (43, 44).

The BS model may be useful for some qualitative behavior of turbulent quantum fluids, but its assumption of point-like vortex cores and the absence of explicit VRs are severe drawbacks. In dilute BECs, in which during the expansion a single vortex core may be comparable with the dimension of the whole condensate, this model is not expected to be successful.

3.4.2. The Gross–Pitaevskii equation. The GP approximation was formulated independently by Gross (45) and Pitaevskii (46) in 1961. The key assumption of this mean-field model is that all particles are in the same single-particle state. Thus, the whole system can be described by a macroscopic wave function $\psi(\mathbf{r}, t)$, which can be found by solving

$$i\hbar \frac{\partial \psi(\mathbf{r}, t)}{\partial t} = \left[-\frac{\hbar^2}{2m}\nabla^2 + V_{\mathrm{trap}} + g|\psi(\mathbf{r}, t)|^2 \right] \psi(\mathbf{r}, t). \qquad 6.$$

The parameter $g = 4\pi a_s \hbar^2/m$ measures the strength of the interaction, and it is proportional to the s-wave scattering length a_s; the normalization is given by $\int \mathrm{d}^3\mathbf{r}|\psi|^2 = N$. Although the GP model is a mean-field approach, in the limit of a $T = 0$ dilute condensate with two-body repulsive interaction potentials, the GP equation is exact (47, 48).

Contrary to the BS model, VRs are present in the solutions and do not have to be included ad hoc. The GP equation has been used successfully to describe a variety of scenarios (49), and dissipation effects can also be included in it (50). Finally, we should note that methods beyond a mean-field approach are available (51–54). A survey on simulations using the GP model, and several other numerical methods applied to QT, can be found in Reference 55.

We can perform a Madelung transformation to $\psi(\mathbf{r}, t)$ so that $\psi(\mathbf{r}, t) = f(\mathbf{r}, t)\exp[iS(\mathbf{r}, t)]$, where the real functions f and S are associated with the square root of the density and phase of the wave function, respectively. Substituting this into Equation 6 yields two equations corresponding to the real and imaginary components (8),

$$\frac{\partial f^2}{\partial t} = -\frac{\hbar}{m}\nabla \cdot (f^2 \nabla S), \qquad 7.$$

$$-\hbar \frac{\partial S}{\partial t} = -\frac{\hbar^2}{2mf}\nabla^2 f + \frac{1}{2}mv^2 + V_{\mathrm{trap}} + gf^2, \qquad 8.$$

with $v = |\mathbf{v}| = |\hbar\nabla S/m|$. Equation 7 is the continuity equation with $\rho = f^2$ and $\mathbf{j} = \hbar f^2 \nabla S/m$, which shows that the probability $|\psi|^2$ is conserved. The gradient of Equation 8 yields

$$\frac{\partial \mathbf{v}}{\partial t} = -\frac{1}{m\rho}\nabla p - \frac{1}{2}\nabla v^2 + \frac{1}{m}\nabla\left(\frac{\hbar^2}{2m\sqrt{\rho}}\nabla^2\sqrt{\rho}\right) - \frac{1}{m}\nabla V_{\text{trap}}, \qquad 9.$$

WT: wave turbulence

where we identified $p = \rho^2 g/2$. Only one term contains $\hbar$, and it is referred to as quantum pressure, which dominates its classical counterpart only for distances of the order of (or less than) the healing length. Neglecting this term yields the dissipation-free Navier–Stokes equation, Equation 3, with $\nu = 0$. It has been pointed out (56) that S is a multivalued field, thus the chain rule of differentiation cannot be applied to $\exp[iS]$. Indeed, the curl of Equation 9 would lead us to believe that vorticity has no dynamics, $\partial\boldsymbol{\omega}/\partial t = 0$. In Reference 56, the author derives exact hydrodynamic equations that present superfluid behavior and include vorticity dynamics.

3.5. Wave Turbulence

We have discussed turbulence resulting from the motion and interaction of vortices. However, some processes in BECs involve interacting dispersive waves giving rise to turbulence, such as is the case of sound waves. We associate the term wave turbulence (WT) to these types of phenomena. This process is also a power-law cascade in the energy spectrum (57). When the equations of motion describe weakly nonlinear dispersion, an analytical description is possible (58). Sound waves are small amplitude excitations to a macroscopic wave function of the condensate. Keeping only the smallest nonlinearity (59) it is possible to analyze plane-wave solutions and their nonlinear corrections (60). The result is a three-wave process that allows the existence of a steady state characterized by an energy cascade (58, 61). In the long-wavelength regime, the energy spectrum is of the Zakharov–Sagdeev type, $E \propto k^{-3/2}$ (58).

WT may also arise from the vibratory motion of vortex lines, known as Kelvin waves. The first theory formulated to explain this type of phenomena involved a six-wave process (35). Later, Nazarenko pointed out that two different cascades can occur simultaneously in WT if an even number of waves are involved (58). A direct energy cascade flows from large to small length scales, and there is also an inverse wave action. Within the Kozik–Svistunov theory (35), $E \propto k^{-7/5}$ for the direct process, whereas $E \propto k^{-1}$ for the inverse action. Kelvin waves occur in classical and quantum fluids (35, 62). In trapped BECs, they have been observed as the result of the decay of quadrupole modes (63). Studies suggest that they may be responsible for the energy transfer between the scales of intervortex separation down to vortex core sizes (64–66). This feature is present in simulations (65) using the BS model (see Section 3.4.1), which does not include a compressible velocity field. The conclusion is that the cascade enabled by Kelvin waves involves only vortex energy, independent of phonons or other collective modes.

3.6. Vortex Reconnections

Experiments with BECs generate a large number of vortices that reconnect and tangle with each other (4, 67). Many experimental techniques for the creation of vortices in dilute BECs are available (68, 69). A VR corresponds to the approximation of two vortex lines, which then connect and exchange tails. They are largely responsible for the energy transfer between different scales; thus, VRs are of great importance to the study of QT (70). In Reference 56, the creation or annihilation of a pair of touching vortex lines obeys the power law $x \propto t^{1/2}$, where x is the distance between the lines and t is the time, which has also been observed in experiments (71) and simulations (72).

In liquid He, VRs have been observed in detail (73), whereas its observation in trapped BECs is much more recent (74). VRs release kinetic energy, and they concentrate vibrations on individual vortex cores, which in turn can be carried by helical Kelvin waves. This is related to an open question at the heart of QT: the mechanism behind dissipation of $T = 0$ frictionless fluids (64). Vinen proposed that high-frequency oscillations of a vortex core can produce phonons in order to dissipate energy in an inviscid fluid (75).

3.7. Quantum Turbulence in Two Dimensions

We already mentioned that CT in 2D is very different from the three-dimensional case. Unlike the classical case, where the two-dimensional character is often an approximation to a three-dimensional problem, truly two-dimensional systems can be realized with BECs by exploring the experimental control on the trapping potentials. This makes dilute cold gases the ideal systems to study two-dimensional QT (2D QT) (2). Kelvin waves, the cornerstone for QT decay in 3D, are not present in 2D, because vortices are zero-dimensional objects in a plane.

The incompressible kinetic energy spectrum of the two-dimensional turbulent regime, for a quasiclassical system with a relatively large D/ξ, is given by $E \propto k^{-3}$ for $k \gg 1/\xi$, and $E \propto k^{-5/3}$ for $k < 1/\xi$ (76). In Section 3.3.1, we stated that the classical energy spectrum is proportional to k^{-3} for larger momenta due to a direct enstrophy cascade. Although in the quantum case the exponent is the same, the mechanism behind it is completely different. The k^{-3} scaling is the result of the velocity field profile of the quantized vortices, which are also responsible for the enstrophy to be proportional to the number of vortices (2, 76). The possibility of a vortex–antivortex pair annihilation causes the enstrophy not to be an inviscid quantity. This feature of fluctuating number of vortices is highlighted in GP simulations of Reference 77. Another study employed simulations of a purely incompressible fluid and found that the inverse energy cascade takes place only for systems with moderate dissipation (78). Further evidence for the inverse energy cascade includes dynamical simulations of a forced homogeneous system in which the $k^{-5/3}$ scaling was observed as well as clusters of vortices with the same sign (79).

The first investigations of QT in BECs looked for quasiclassical characteristics (80). Unlike the homogeneous case, trapped BECs tend to prevent large-scale motion, so that Vinen turbulence is usually observed. For example, in Reference 81 the stirring of a BEC, which was happening at distances of the order of the healing length, was unable to produce the growth of vortex clustering due to the system size. When the Kolmogorov scaling can be seen, usually it is for regions less than a decade (82), again due to the lack of range of scales available.

Another obstacle to observing QT in 2D is the vortex–antivortex pair annihilation, which largely prevents vortex clustering. Experimental protocols for vortex generation end up producing roughly the same number of positive- and negative-charge vortices (23, 67, 83). Techniques for successive nucleation of vortices have been proposed (84). Results of simulations in a large, homogeneous BEC clearly show that vortex annihilation is a four-vortex process (85).

3.8. Miscellanea

The most common picture of QT in trapped quantum gases involves a single-component spinless bosonic fluid. However, experiments and theoretical investigations that depart from this picture have been carried out. These may shed light on aspects of QT that were not explored before.

3.8.1. Bosonic mixtures. So far, we have limited ourselves to the discussion of single-component BECs. However, QT can also be studied in a mixture of two (or more) bosonic species,

with substantially different behavior. Theoretical investigations of counterflow turbulence have been carried out employing a mixture of two bosonic species (86, 87). This would be the analog of QT in ^{4}He at sufficiently high temperatures when both the normal and superfluid components are turbulent. QT can also be studied using condensates with particles possessing a spin degree of freedom (88, 89). The main difference to a regular mixture of bosonic species is that the population of each spin state is not constant due to spin-exchange collisions. For more details about spin turbulence, the reader is referred to Reference 90 and references therein.

BCS: Bardeen–Cooper–Schrieffer

3.8.2. Fermionic gases. Superfluidity can also be achieved in fermionic systems, which is explained through the Bardeen–Cooper–Schrieffer (BCS) theory of condensation of Cooper pairs into bosonic-like particles (91). Interest in cold atomic fermionic gases is further augmented by the BEC-BCS crossover (92), where the interparticle interactions can be tuned so that the fermion pairs can change their size from tightly bound dimers (BEC) to many times the interparticle distance at the BCS side, passing through the strongly interacting unitary regime. A landmark was the production of vortex lattices, throughout the crossover, in an ultracold ^{6}Li gas, demonstrating superfluidity (93). The first question that arises is whether QT is possible in fermionic gases and, if so, in which regimes of BEC-BCS crossover turbulence emerges (94). Apparently, QT is possible in the unitary Fermi gas (95), and VRs were studied in this regime (96). The microscopic structure of vortices in cold atomic fermionic gases has been studied throughout the BEC-BCS crossover and in the unitary Fermi gas (97, 98).

3.8.3. Neutron stars. Many problems in nuclear physics are related to QT. Because protons and neutrons are spin-1/2 particles, QT of fermionic gases is of interest. In particular, QT may hold the key to a mystery in nuclear astrophysics, the pulsar glitches. They correspond to sudden increases in the spinning of neutron stars while they continually lose angular momentum. It has been suggested that the outer core of a neutron star is in a turbulent state, and that the Reynolds number is related to the glitches (99, 100). The main challenge in this problem is the disparity between the femtometer scale of vortex cores and the kilometer scale of neutron stars; however, progress has been made toward developing a mean field description (101). As is the case with turbulence in trapped BECs, we need a better understanding of microscopic processes, such as VRs, that take place in the crust of neutron stars. Even the study of a single vortex line in neutron matter is an active topic of research (102).

4. EXPERIMENTS

The study of quantized vortices and QT has increased in intensity with the realization of weakly interacting dilute atomic BECs (9, 11). Stimulated largely by the high degree of control that is available within these quantum gases (103–106), BECs have been used to investigate QT both experimentally and theoretically. The ability to directly resolve the structure of individual vortices, and hence the dynamics of a turbulent vortex tangle (63, 64, 74), opens the possibility of studying problems that may be relevant to our general understanding of turbulence.

4.1. The São Carlos Group

We start by reviewing some of our contributions, both theoretical and experimental, to the field of QT, and we show how they are related to research being conducted worldwide. In 2009, the São Carlos group was responsible for the first evidence of QT in trapped dilute atomic BECs (4). The experiment consisted of a small vortex tangle created in a harmonically trapped BEC through the combination of rotation and an external oscillating perturbation (4, 107).

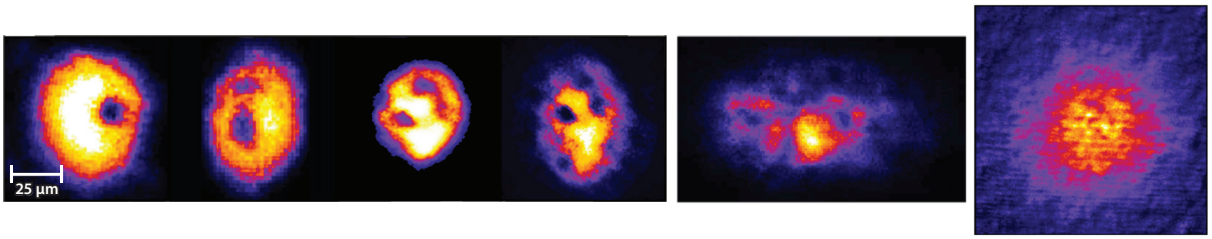

Figure 2

Phases of the excited Bose–Einstein condensate, according to the time and amplitude of the applied external oscillatory magnetic field. Panels show (*a*) regular vortices, (*b*) turbulent cloud, and (*c*) granulation. Panels adapted from Reference 108.

Different regimes were observed according to the strength and duration of the external oscillatory potential (5) (**Figure 2**). For small amplitude excitations, the only effect was a bending of the main axis of the cloud, irrespective of the duration of the oscillation. Increasing the amplitude of the oscillation caused regular vortices to be nucleated, with the number of vortices increasing monotonically with the application time of the external excitation. Increasing the excitation time further led to a turbulent vortex regime. At very long hold times, the condensate fragmented or granulated, signalizing the decay of the turbulence.

4.1.1. Finite-size system. Currently, the BEC systems that can be created in the laboratory contain a small number of atoms (a few hundred thousand), and hence do not sustain the number of quantum vortices present in He experiments. This brings to light the question about the Kolmogorov's scaling, i.e., whether it still holds in the small range of lengths available. Despite of the limited number of vortices present in trapped BECs, numerical simulations of these systems (66, 109–111) suggest that the kinetic energy is distributed over the length scales in agreement with the $k^{-5/3}$ Kolmogorov scaling observed in ordinary turbulence.

Attempts to model analytically the transition to turbulence in these finite systems are available in the literature. The transition from vortices to the turbulent regime could be established assuming a critical number of vortices, according to the size of the sample (112) and to the input energy coming from the external excitation. In Reference 113, the authors performed numerical calculations to reproduce our experimental conditions. According to the excitation parameters, the perturbed system was classified by a phase diagram. Particular aspects of the granular phase were explored (114).

4.1.2. Self-similar expansion. The most common diagnostic of trapped atomic clouds is done by imaging them, not in the trap, but after some time of free expansion. That easily distinguishes a thermal from a Bose-condensed cloud. A thermal cloud shows a Gaussian density profile that evolves to an isotropic density distribution at long times of expansion. The quantum cloud, in contrast, shows a profile that initially reflects the shape of the confining trap, the Thomas–Fermi regime. In a cigar-shaped trap, for example, the BEC cloud expands faster in the radial than in the axial direction. That causes the signature inversion of the BEC cloud aspect ratio during the free expansion.

Considering now a turbulent BEC cloud, besides the evidence of the tangle vortices configuration in the density profile (atomic depletion in the absorption image), the cloud free-expansion dynamics also differs owing to the presence of vorticity. In fact, for the cigar-shape trap used in Reference 4, the turbulent condensate expands with a nearly constant aspect ratio once released from its confinement.

To characterize the anomalous expansion of the turbulent sample, a generalized Lagrangian approach was applied in Reference 115. The kinetic energy contribution of a tangle vortex configuration was added to the system Lagrangian, and the resulting Euler–Lagrange equations described the dynamics of the cloud.

TOF: time-of-flight

4.1.3. Atomic-turbulence and speckle-fields. BECs and atom lasers are examples of coherent matter-wave systems. By contrast, an optical speckle pattern can be created by the mutual interference of many light waves of the same frequency, with different amplitudes and phases, giving rise to a random light map. Very interesting work (116) draws a parallel between a ground-state/turbulent BEC with the propagation of an optical Gaussian beam/elliptical speckle light map.

The researchers analyzed mainly two characteristics of the spatial disorder of the systems. First, measurements of the aspect ratios of regular and turbulent BECs were performed. For standard BECs there is an inversion of the aspect ratio of the cloud in time-of-flight (TOF) measurements, whereas in the turbulent case there is a self-similar expansion, without ever inverting its aspect ratio (115). For a coherent Gaussian beam, there is an inversion of the aspect ratio of the waists, whereas it is preserved in the propagation of the elliptical speckle light map, just as is the case with the BEC counterparts. The second property that was investigated was the coherence in both systems. It was found that the correlations in regular BECs resemble the ones in the Gaussian beam, whereas the same is true for the turbulent BEC and speckle beam pair. This duality opens the possibility of improving our understanding of QT by looking at statistical atom optics.

4.1.4. Momentum distribution of a turbulent trapped BEC. To investigate turbulence experimentally, atoms are held for tens of milliseconds in the trap, after the drive has been terminated, and then they are released for imaging. The atoms are measured by a TOF absorption image technique. In Reference 6, TOF was used to probe the momentum distribution of a turbulent BEC cloud, assuming a ballistic expansion for the atoms. They found a power-law behavior for the momentum distribution of $n(k) \propto k^{-2.9}$ (**Figure 3**).

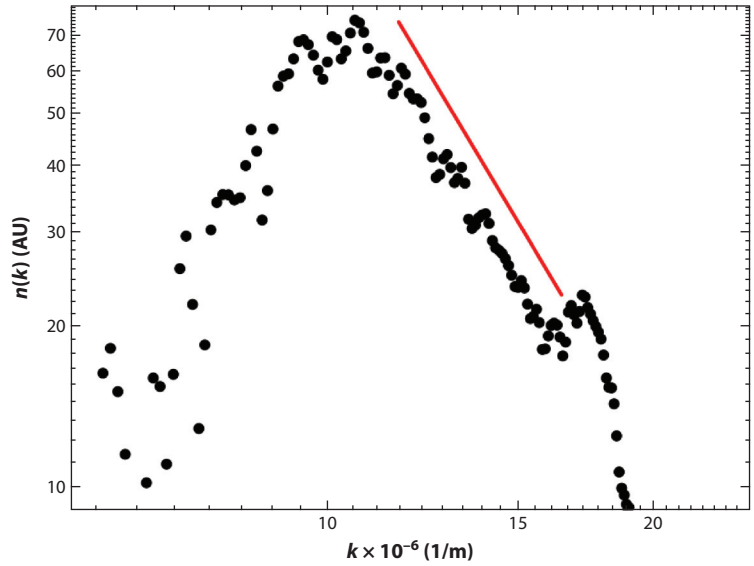

Figure 3

Three-dimensional momentum distribution for a turbulent cloud. The curve corresponds to a line with slope −2.9. Figure adapted from Reference 6 by permission of IOP Publishing. ©Astro Ltd. All rights reserved.

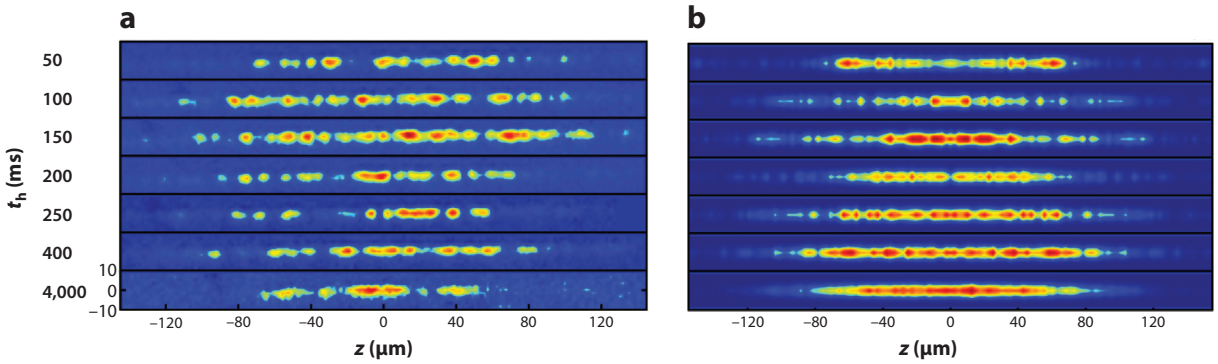

Figure 4

Response of an elongated Bose–Einstein condensate to modulated interactions: (*a*) experiment and (*b*) numerical simulations. Granulation is remarkably persistent in time after the modulation is turned off, and its structure is random between different experimental runs. Figure adapted from Reference 118.

The momentum distribution is extracted from measurements of the absorption image of the expanded cloud. The projected image is a distorted two-dimensional shadow of the real atomic distribution. As a result, the spatial density has contributions from many wave numbers along the path of the imaging light. As the interaction is assumed to be negligible, the ballistically expanding atoms allow for an experimental Fourier conversion of the real space density distribution after a TOF to an in situ momentum distribution. The radii of the expanded cloud are converted in momentum shells, and the number of atoms are counted in each shell to construct the momentum distribution of the sample.

Remarkably, the turbulent spectra showed a higher-momentum atomic population that is not present in the spectra of a normal BEC. In particular, this unusual region of the spectra showed a distribution that decreases monotonically with the momentum, and its slope in a logarithmic scale can be associated to a power law.

4.1.5. Collective modes, Faraday waves, and granulation. In Reference 117, a gas of ^{7}Li atoms was cooled to nearly zero temperature, and the collective modes of an elongated BEC were studied with the modulation of the atomic scattering length. Different regimes appeared by varying the frequency and modulation strength of the external magnetic field. This was explored further, both experimentally and theoretically, in Reference 118. Particularly, for modulation frequencies near twice the trap frequency, longitudinal surface waves are generated resonantly (parametrically). The dispersion of these waves, also called resonant (119) or Faraday waves (120, 121), is well reproduced by a mean-field theory. Otherwise, far from the resonances (lower modulation frequencies), increasing the modulation strength brings an irregular granulated distribution in the condensate density (**Figure 4**). The correlations of this granulated phase could be described with a beyond mean-field theory,[1] which characterizes the large quantum fluctuations of this peculiar regime.

4.2. Two-Dimensional Quantum Turbulence

Because there is a lack of experimental correspondence, previous numerical studies on 2D QT, which dealt with the energy spectra and vortex dynamics, did not establish any connection with

[1] `MCTDH-X` is the time-dependent multiconfigurational Hartree for indistinguishable particles software, available at **http://ultracold.org/**.

two-dimensional CT. Recently, the experiments (23, 122) showed that even a trapped superfluid sample exhibits many similarities to that expected from the two-dimensional CT, extending the universality of two-dimensional turbulence.

To experimentally generate 2D QT, a combined optical–magnetic confinement creates highly oblate BEC, with the turbulent flow resulting from the effective stirring of the center region of the condensate by a repulsive optical potential. This external perturbation induces randomly distributed nucleation of vortices. Then the trap is turned off, and the expanded BEC provides the absorption image of the vortices.

In Reference 122, the authors investigated, experimentally and numerically, the forced and decaying 2D QT in a BEC. It was demonstrated that the disordered vortex distributions of 2D QT can be sustained in spite of the vortex–antivortex annihilation. Their observations are indicators of the energy transport from small to large length scales, corresponding to the inverse energy cascade. The thermal relaxation of superfluid turbulence in 2D, based on evidence of the vortex–antivortex annihilation mechanism, was investigated in Reference 23. These authors showed the essential role played by vortex–antivortex pairs in 2D QT, characterizing the relaxation of the turbulent condensate through the decay rates of the vortex number.

5. CHALLENGES AND OPEN QUESTIONS

Trapped superfluid BECs show turbulent behavior. Evidence of energy cascades with power-law behavior have been measured in experiments and supported by theoretical models. The amount of control that can be exerted on BEC experiments makes them excellent candidates to investigate QT. Nevertheless, several aspects of this phenomenon need experimental investigation and theoretical clarification. In the following, we summarize some of the challenges that the field must face.

- **Tuning the interactions:** Throughout this manuscript, we pointed out several limitations due to the range of available length scales in experiments. A quick estimate of $\log(D/\xi)$, involving the system size D and the healing length ξ, shows that experiments are limited to one or two orders of magnitude at best. However, interactions in trapped BECs can be controlled through Feshbach resonances (103) to produce smaller healing lengths and larger cloud radii at the same time, improving the range of scale lengths available. How would turbulence formation, decay, and scaling laws, react in different interacting environments? Many other questions could be investigated as one studies turbulence in tunable BECs.
- **Finite size:** Currently, the dilute BECs that can be created in the laboratory contain a small number of atoms, hence they do not sustain the number of quantum vortices present in He experiments. Fundamental questions exist concerning the extent to which turbulence can be generated and observed in such small and inhomogeneous systems.
- **Inhomogeneity:** Trapped quantum gases are not homogeneous systems. What is the influence of this on characteristics of QT in these systems? Following the release of the trap, turbulence is expected to be isotropic after a sufficiently long time. However, experiments are limited to images a few tens of milliseconds after the trap is turned off. Models that explicitly take into account differences between the homogeneous and isotropic behavior of turbulence in bulk fluids and the experimental conditions of trapped gases could provide some answers. Also, QT in other nonhomogeneous systems, such as piston shock experiments in channel geometries (123), could bring some insight into this question.
- **Probing the turbulent cloud:** Visualization of the turbulent cloud is of paramount importance for advances in the field. Techniques for visualizing the vortex tangle are well

developed in liquid He systems (73), and the same level of detail needs to be achieved in trapped condensates. In this sense, the determination of the kinetic energy spectrum, and thus the associated turbulence mechanism, could benefit from in situ measurements of momentum distributions. The task of extracting the momentum distribution from two-dimensional integrated density profiles of three-dimensional vortex tangles constitutes a huge challenge for understanding QT.

- **Kolmogorov's law:** The verification of the $-5/3$ Kolmogorov's law would be by far one of the most spectacular results toward a universal description of turbulence. However, there are questions one must ask in order to investigate this law in trapped atomic BECs. Does turbulence in BECs achieve the stationary state necessary to the Kolmogorov cascade to be settled? Is the number of vortices in the BEC enough to characterize the Kolmogorov length scales?
- **Vortex turbulence:** Questions are being asked about the role played by VRs in turbulence and about the nonclassical quantum turbulent regime (called Vinen or ultraquantum turbulence), which is different from ordinary turbulence in terms of energy spectrum and decay. The wide range of length scales available in turbulence gives rise to energy cascades with power-law behavior. Measuring the exponent does not mean that the mechanism behind it is understood, especially when models predict exponents spaced closely together. Kolmogorov turbulence assumes vortex bundles; however, due to the finite size of trapped BECs, their formation is unlikely to happen.
- **Mechanism of vortex tangle generation:** Theoretical simulations point out that a certain degree of dissipation must be introduced in the GP equation in order to generate vortices, the phenomenological dissipative part representing the effects of the thermal cloud (110, 124–126). In previous work, there is evidence of counter-flow in excited BECs, with thermal and condensate components moving out of phase and against each other (127). The presence of vortices in the interface between the BEC and the thermal cloud has been observed, indicating that the thermal cloud has indeed some degree of contribution in the vortex nucleation. In that sense, the study of vortex generation and evolution to a vortex tangle as a function of the size of the thermal component must be investigated.
- **Generation and decay of turbulence:** What are the most effective and efficient ways to generate turbulence? Does the way in which the turbulence is generated affect the type of turbulence created? Also, one important aspect to characterize in experiments is how turbulence decays. To observe this process, one needs high-resolution and nondestructive imaging of the trapped cloud. How can one quantify this decay experimentally, i.e., what are the experimental observables that allow quantification of decay rates?
- **"Exotic" systems:** Systems that depart from the standard single-component BEC, which is usually employed in experiments and simulations, may shed light on aspects of QT that have not been explored yet. Recently, turbulence in a dipolar Bose gas has been achieved (128), opening the possibility to study QT with long-range interactions. Another example consists of bosonic mixtures of two (129–142), or possibly more, species that could be used in QT experiments. Besides the intrinsic differences between the behavior of the two systems, one species could be used as a means to visualize the other. Another possibility for multicomponent gases is using BECs with spin degrees of freedom. Though much of this review is based on bosonic fluids, fermionic gases can also display superfluidity. The study of QT in cold atomic Fermi gases is still incipient, and much remains to be done.
- **Change in the dimensionality:** A highly oblate, but still three-dimensional, BEC may suppress superfluid flow along the tight-confining direction, providing two-dimensional

superfluid vortex dynamics. Hence, two-dimensional turbulence can be obtained (143). These systems open the possibility of investigating transitions between QT in 2D and 3D.

- **Beyond mean-field theory:** We should also note that much of the theoretical framework relies on mean-field theories. Effects beyond the mean field need to be investigated to either show that the GP model is valid or pinpoint its limitations.

DISCLOSURE STATEMENT

The authors are not aware of any affiliations, memberships, funding, or financial holdings that might be perceived as affecting the objectivity of this review.

ACKNOWLEDGMENTS

We thank M.C. Tsatsos, P.E.S. Tavares, A. Cidrim, A.R. Fritsch, and C.F. Barenghi for useful discussions. This work was supported by the São Paulo Research Foundation (FAPESP) under the grants 2018/09191-7 and 2013/07276-1. We also thank Centro de Pesquisa em Ótica e Fotônica (CePOF) for their financial support. F.E.A.S. acknowledges CNPq for support through Bolsa de Produtividade em Pesquisa No. 305586/2017-3.

LITERATURE CITED

1. Tsubota M. 2008. *J. Phys. Soc. Jpn.* 77:111006
2. White AC, Anderson BP, Bagnato VS. 2014. *PNAS* 111:4719–26
3. Tsatsos MC, Tavares PE, Cidrim A, Fritsch AR, Caracanhas MA, et al. 2016. *Phys. Rep.* 622:1–52
4. Henn EAL, Seman JA, Roati G, Magalhães KMF, Bagnato VS. 2009. *Phys. Rev. Lett.* 103:045301
5. Seman J, Henn E, Shiozaki R, Roati G, Poveda-Cuevas F, et al. 2011. *Laser Phys. Lett.* 8:691–96
6. Thompson KJ, Bagnato GG, Telles GD, Caracanhas MA, dos Santos FEA, Bagnato VS. 2013. *Laser Phys. Lett.* 11:015501
7. Navon N, Gaunt AL, Smith RP, Hadzibabic Z. 2016. *Nature* 539:72
8. Pethick CJ, Smith H. 2008. *Bose-Einstein Condensation in Dilute Gases*. Cambridge, UK: Cambridge Univ. Press. 2nd ed.
9. Anderson MH, Ensher JR, Matthews MR, Wieman CE, Cornell EA. 1995. *Science* 269:198–201
10. Bradley CC, Sackett CA, Tollett JJ, Hulet RG. 1995. *Phys. Rev. Lett.* 75:1687–90
11. Davis KB, Mewes MO, Andrews MR, van Druten NJ, Durfee DS, et al. 1995. *Phys. Rev. Lett.* 75:3969–73
12. Balibar S. 2007. *J. Low Temp. Phys.* 146:441–70
13. Kapitza P. 1938. *Nature* 141:74
14. Allen J, Misener A. 1938. *Nature* 141:75
15. London F. 1938. *Nature* 141:643
16. Tisza L. 1938. *Nature* 141:913
17. Balibar S. 2017. *C. R. Phys.* 18:586–91
18. Eyink GL, Sreenivasan KR. 2006. *Rev. Mod. Phys.* 78:87–135
19. Feynman R. 1955. In *Progress in Low Temperature Physics*, ed. C Gorter, Vol. 1, pp. 17–53. New York: Intersci. Publ.
20. Kawaguchi Y, Ohmi T. 2004. *Phys. Rev. A* 70:043610
21. Barenghi C. 1982. *Experiments on quantum turbulence*. PhD Thesis, Univ. Or., Eugene
22. Donnelly RJ, Swanson CE. 1986. *J. Fluid Mech.* 173:387–429
23. Kwon WJ, Moon G, Choi JY, Seo SW, Shin YI. 2014. *Phys. Rev. A* 90:063627
24. Stagg GW, Allen AJ, Parker NG, Barenghi CF. 2015. *Phys. Rev. A* 91:013612
25. Nore C, Abid M, Brachet ME. 1997. *Phys. Rev. Lett.* 78:3896–99
26. Hall HE, Vinen WF. 1956. *Proc. R. Soc. Lond. Ser. A. Math. Phys. Sci.* 238:204–14

27. Hall HE, Vinen WF. 1956. *Proc. R. Soc. Lond. Ser. A. Math. Phys. Sci.* 238:215–34
28. Baggaley AW, Laurie J, Barenghi CF. 2012. *Phys. Rev. Lett.* 109:205304
29. Walmsley PM, Golov AI. 2008. *Phys. Rev. Lett.* 100:245301
30. Baggaley AW, Barenghi CF, Sergeev YA. 2012. *Phys. Rev. B* 85:060501
31. Zamora-Zamora R, Adame-Arana O, Romero-Rochin V. 2015. *J. Low Temp. Phys.* 180:109–25
32. Kobayashi M, Tsubota M. 2005. *Phys. Rev. Lett.* 94:065302
33. Volovik GE. 2003. *J. Exp. Theor. Phys. Lett.* 78:533–37
34. Baggaley AW, Sherwin LK, Barenghi CF, Sergeev YA. 2012. *Phys. Rev. B* 86:104501
35. Kozik E, Svistunov B. 2004. *Phys. Rev. Lett.* 92:035301
36. L'vov VS, Nazarenko S. 2010. *J. Exp. Theor. Phys. Lett.* 91:428–34
37. Krstulovic G. 2012. *Phys. Rev. E* 86:055301
38. Baggaley AW, Laurie J. 2014. *Phys. Rev. B* 89:014504
39. Kondaurova L, L'vov V, Pomyalov A, Procaccia I. 2014. *Phys. Rev. B* 90:094501
40. L'vov VS, Nazarenko SV, Rudenko O. 2007. *Phys. Rev. B* 76:024520
41. Kozik E, Svistunov B. 2008. *Phys. Rev. B* 77:060502
42. L'vov VS, Nazarenko SV, Rudenko O. 2008. *J. Low Temp. Phys.* 153:140–61
43. Schwarz KW. 1985. *Phys. Rev. B* 31:5782–804
44. Barenghi CF, Donnelly RJ, Vinen W, eds. 2001. *Quantized Vortex Dynamics and Superfluid Turbulence*, Vol. 571. Berlin/Heidelberg: Springer-Verlag
45. Gross EP. 1961. *Il Nuovo Cimento (1955–1965)* 20:454–77
46. Pitaevskii L. 1961. *Sov. Phys. JETP* 13:451–54
47. Lieb EH, Seiringer R, Yngvason J. 2000. *Phys. Rev. A* 61:043602
48. Lieb EH, Seiringer R. 2002. *Phys. Rev. Lett.* 88:170409
49. Dalfovo F, Giorgini S, Pitaevskii LP, Stringari S. 1999. *Rev. Mod. Phys.* 71:463–512
50. Tsubota M, Kasamatsu K, Ueda M. 2002. *Phys. Rev. A* 65:023603
51. Streltsov AI, Alon OE, Cederbaum LS. 2006. *Phys. Rev. A* 73:063626
52. Streltsov AI, Alon OE, Cederbaum LS. 2007. *Phys. Rev. Lett.* 99:030402
53. Alon OE, Streltsov AI, Cederbaum LS. 2008. *Phys. Rev. A* 77:033613
54. Wells T, Lode AUJ, Bagnato VS, Tsatsos MC. 2015. *J. Low Temp. Phys.* 180:133–43
55. Tsubota M, Fujimoto K, Yui S. 2017. *J. Low Temp. Phys.* 188:119–89
56. dos Santos FEA. 2016. *Phys. Rev. A* 94:063633
57. Fujimoto K, Tsubota M. 2015. *Phys. Rev. A* 91:053620
58. Nazarenko S. 2011. *Wave Turbulence*, Vol. 825, *Lect. Notes Phys.* Heidelberg: Springer Sci. Bus. Media
59. Kevrekidis PG, Frantzeskakis DJ, Carretero-González R, eds. 2008. *Emergent Nonlinear Phenomena in Bose-Einstein Condensates: Theory and Experiment*, Vol. 45. Berlin/Heidelberg: Springer-Verlag
60. Lvov Y, Nazarenko S, West R. 2003. *Phys. D: Nonlinear Phenomena* 184:333–51
61. Zakharov VE, L'vov VS, Falkovich G. 1992. *Kolmogorov Spectra of Turbulence I.* Berlin/Heidelberg: Springer-Verlag
62. Nazarenko S. 2006. *J. Exp. Theor. Phys. Lett.* 83:198–200
63. Bretin V, Rosenbusch P, Chevy F, Shlyapnikov GV, Dalibard J. 2003. *Phys. Rev. Lett.* 90:100403
64. Fonda E, Meichle DP, Ouellette NT, Hormoz S, Lathrop DP. 2014. *PNAS* 111:4707–10
65. Kivotides D, Vassilicos JC, Samuels DC, Barenghi CF. 2001. *Phys. Rev. Lett.* 86:3080–83
66. Tsubota M. 2009. *J. Phys.: Condens. Matter* 21:164207
67. White AC, Proukakis NP, Barenghi CF. 2014. *J. Phys.: Conf. Ser.* 544:012021
68. Fetter AL. 2009. *Rev. Mod. Phys.* 81:647–91
69. Fetter AL. 2010. *J. Low Temp. Phys.* 161:445–59
70. Serafini S, Galantucci L, Iseni E, Bienaimé T, Bisset RN, et al. 2017. *Phys. Rev. X* 7:021031
71. Paoletti M, Fisher ME, Lathrop D. 2010. *Phys. D: Nonlinear Phenomena* 239:1367–77
72. Siggia ED, Pumir A. 1985. *Phys. Rev. Lett.* 55:1749–52
73. Bewley GP, Lathrop DP, Sreenivasan KR. 2006. *Nature* 441:588
74. Serafini S, Barbiero M, Debortoli M, Donadello S, Larcher F, et al. 2015. *Phys. Rev. Lett.* 115:170402
75. Vinen WF. 2000. *Phys. Rev. B* 61:1410–20

76. Bradley AS, Anderson BP. 2012. *Phys. Rev. X* 2:041001
77. Numasato R, Tsubota M, L'vov VS. 2010. *Phys. Rev. A* 81:063630
78. Billam TP, Reeves MT, Bradley AS. 2015. *Phys. Rev. A* 91:023615
79. Reeves MT, Billam TP, Anderson BP, Bradley AS. 2013. *Phys. Rev. Lett.* 110:104501
80. Parker NG, Adams CS. 2005. *Phys. Rev. Lett.* 95:145301
81. White AC, Barenghi CF, Proukakis NP. 2012. *Phys. Rev. A* 86:013635
82. Reeves MT, Anderson BP, Bradley AS. 2012. *Phys. Rev. A* 86:053621
83. Neely TW, Samson EC, Bradley AS, Davis MJ, Anderson BP. 2010. *Phys. Rev. Lett.* 104:160401
84. Sasaki K, Suzuki N, Saito H. 2010. *Phys. Rev. Lett.* 104:150404
85. Baggaley AW, Barenghi CF. 2018. *Phys. Rev. A* 97:033601
86. Takeuchi H, Ishino S, Tsubota M. 2010. *Phys. Rev. Lett.* 105:205301
87. Ishino S, Tsubota M, Takeuchi H. 2011. *Phys. Rev. A* 83:063602
88. Mueller EJ, Ho TL, Ueda M, Baym G. 2006. *Phys. Rev. A* 74:033612
89. Stamper-Kurn DM, Ueda M. 2013. *Rev. Mod. Phys.* 85:1191–244
90. Tsubota M, Fujimoto K. 2014. *J. Phys.: Conf. Ser.* 497:012002
91. Bardeen J, Cooper LN, Schrieffer JR. 1957. *Phys. Rev.* 108:1175–204
92. Randeria M, Taylor E. 2014. *Annu. Rev. Condens. Matter Phys.* 5:209–32
93. Zwierlein MW, Abo-Shaeer JR, Schirotzek A, Schunck CH, Ketterle W. 2005. *Nature* 435:1047
94. Bulgac A, Forbes MM, Wlazłowski G. 2016. *J. Phys. B: Atomic, Mol. Opt. Phys.* 50:014001
95. Wlazłowski G, Quan W, Bulgac A. 2015. *Phys. Rev. A* 92:063628
96. Wlazłowski G, Bulgac A, Forbes MM, Roche KJ. 2015. *Phys. Rev. A* 91:031602
97. Madeira L, Vitiello SA, Gandolfi S, Schmidt KE. 2016. *Phys. Rev. A* 93:043604
98. Madeira L, Gandolfi S, Schmidt KE. 2017. *Phys. Rev. A* 95:053603
99. Peralta C, Melatos A, Giacobello M, Ooi A. 2006. *Astrophys. J.* 651:1079–91
100. Link B, Melatos A. 2013. *MNRAS* 437:21–31
101. Khomenko V, Haskell B. 2018. *Publ. Astron. Soc. Aust.* 35:e020
102. Madeira L, Gandolfi S, Schmidt KE, Bagnato VS. 2019. *Phys. Rev. C*. Accepted. arXiv:1903.06724
103. Inouye S, Andrews MR, Stenger J, Miesner HJ, Stamper-Kurn DM, Ketterle W. 1998. *Nature* 392:151–54
104. Görlitz A, Vogels JM, Leanhardt AE, Raman C, Gustavson TL, et al. 2001. *Phys. Rev. Lett.* 87:130402
105. Bloch I, Dalibard J, Zwerger W. 2008. *Rev. Mod. Phys.* 80:885–964
106. Henderson K, Ryu C, MacCormick C, Boshier MG. 2009. *New J. Phys.* 11:043030
107. Henn EAL, Seman JA, Ramos ERF, Caracanhas M, Castilho P, et al. 2009. *Phys. Rev. A* 79:043618
108. Shiozaki RF. 2013. *Quantum turbulence and thermodynamics on a trapped Bose-Einstein condensate*. PhD Thesis, Univ. São Paulo, São Paulo, Brazil
109. Berloff NG, Svistunov BV. 2002. *Phys. Rev. A* 66:013603
110. Kobayashi M, Tsubota M. 2007. *Phys. Rev. A* 76:045603
111. Nowak B, Sexty D, Gasenzer T. 2011. *Phys. Rev. B* 84:020506(R)
112. Shiozaki R, Telles G, Yukalov V, Bagnato V. 2011. *Laser Phys. Lett.* 8:393–97
113. Yukalov VI, Novikov AN, Bagnato VS. 2015. *J. Low Temp. Phys.* 180:53–67
114. Yukalov VI, Novikov AN, Bagnato VS. 2014. *Laser Phys. Lett.* 11:095501
115. Caracanhas M, Fetter AL, Baym G, Muniz SR, Bagnato VS. 2013. *J. Low Temp. Phys.* 170:133–42
116. Tavares PES, Fritsch AR, Telles GD, Hussein MS, Impens F, et al. 2017. *PNAS* 114:12691–95
117. Pollack SE, Dries D, Hulet RG, Magalhães KMF, Henn EAL, et al. 2010. *Phys. Rev. A* 81:053627
118. Nguyen JHV, Tsatsos MC, Luo D, Lode AUJ, Telles GD, et al. 2019. *Phys. Rev. X* 9:011052
119. Nicolin AI. 2011. *Phys. Rev. E* 84:056202
120. Nicolin AI, Carretero-González R, Kevrekidis PG. 2007. *Phys. Rev. A* 76:063609
121. Engels P, Atherton C, Hoefer MA. 2007. *Phys. Rev. Lett.* 98:095301
122. Neely TW, Bradley AS, Samson EC, Rooney SJ, Wright EM, et al. 2013. *Phys. Rev. Lett.* 111:235301
123. Mossman ME, Hoefer MA, Julien K, Kevrekidis PG, Engels P. 2018. *Nat. Commun.* 9:4665
124. Proukakis NP, Jackson B. 2008. *J. Phys. B: Atomic, Mol. Opt. Phys.* 41:203002
125. White AC, Barenghi CF, Proukakis NP, Youd AJ, Wacks DH. 2010. *Phys. Rev. Lett.* 104:075301

126. Baggaley AW, Barenghi CF. 2011. *Phys. Rev. E* 84:067301
127. Tavares PES, Telles GD, Shiozaki RF, Branco CC, Farias KM, Bagnato VS. 2013. *Laser Phys. Lett.* 10:045501
128. Bland T, Stagg GW, Galantucci L, Baggaley AW, Parker NG. 2018. *Phys. Rev. Lett.* 121:174501
129. Myatt CJ, Burt EA, Ghrist RW, Cornell EA, Wieman CE. 1997. *Phys. Rev. Lett.* 78:586–89
130. Modugno G, Modugno M, Riboli F, Roati G, Inguscio M. 2002. *Phys. Rev. Lett.* 89:190404
131. Papp SB, Pino JM, Wieman CE. 2008. *Phys. Rev. Lett.* 101:040402
132. Thalhammer G, Barontini G, Sarlo LD, Catani J, Minardi F, Inguscio M. 2008. *Phys. Rev. Lett.* 100:210402
133. McCarron DJ, Cho HW, Jenkin DL, Köppinger MP, Cornish SL. 2011. *Phys. Rev. A* 84:011603
134. Pasquiou B, Bayerle A, Tzanova SM, Stellmer S, Szczepkowski J, et al. 2013. *Phys. Rev. A* 88:023601
135. Wacker L, Jørgensen NB, Birkmose D, Horchani R, Ertmer W, et al. 2015. *Phys. Rev. A* 92:053602
136. Ferrier-Barbut I, Delehaye M, Laurent S, Grier AT, Pierce M, et al. 2014. *Science* 345:1035–38
137. Delehaye M, Laurent S, Ferrier-Barbut I, Jin S, Chevy F, Salomon C. 2015. *Phys. Rev. Lett.* 115:265303
138. Yao XC, Chen HZ, Wu YP, Liu XP, Wang XQ, et al. 2016. *Phys. Rev. Lett.* 117:145301
139. DeSalvo BJ, Patel K, Johansen J, Chin C. 2017. *Phys. Rev. Lett.* 119:233401
140. Roy R, Green A, Bowler R, Gupta S. 2017. *Phys. Rev. Lett.* 118:055301
141. Laurent S, Pierce M, Delehaye M, Yefsah T, Chevy F, Salomon C. 2017. *Phys. Rev. Lett.* 118:103403
142. Wu YP, Yao XC, Liu XP, Wang XQ, Wang YX, et al. 2018. *Phys. Rev. B* 97:020506(R)
143. Rooney SJ, Blakie PB, Anderson BP, Bradley AS. 2011. *Phys. Rev. A* 84:023637